ORIGINAL RESEARCH

Intermittent Hypoxia Augments Pulmonary Vasoconstrictor Reactivity through PKCβ/Mitochondrial Oxidant Signaling

Jessica B. Snow, Charles E. Norton, Michelle A. Sands, Laura Weise-Cross, Simin Yan, Lindsay M. Herbert, Joshua R. Sheak, Laura V. Gonzalez Bosc, Benjimen R. Walker, Nancy L. Kanagy, Nikki L. Jernigan, and Thomas C. Resta

Vascular Physiology Group, Department of Cell Biology and Physiology, University of New Mexico Health Sciences Center, Albuquerque, New Mexico

ORCID ID: 0000-0001-7505-4909 (L.V.G.B.).

Abstract

Pulmonary vasoconstriction resulting from intermittent hypoxia (IH) contributes to pulmonary hypertension (pHTN) in patients with sleep apnea (SA), although the mechanisms involved remain poorly understood. Based on prior studies in patients with SA and animal models of SA, the objective of this study was to evaluate the role of PKCβ and mitochondrial reactive oxygen species (mitoROS) in mediating enhanced pulmonary vasoconstrictor reactivity after IH. We hypothesized that PKCβ mediates vasoconstriction through interaction with the scaffolding protein PICK1 (protein interacting with C kinase 1), activation of mitochondrial ATP-sensitive potassium channels (mitoK$_{ATP}$), and stimulated production of mitoROS. We further hypothesized that this signaling axis mediates enhanced vasoconstriction and pHTN after IH. Rats were exposed to IH or sham conditions (7 h/d, 4 wk). Chronic oral administration of the antioxidant Tempol or the PKCβ inhibitor LY-333531 abolished IH-induced increases in right ventricular systolic pressure and right ventricular hypertrophy. Furthermore, scavengers of O_2^- or mitoROS prevented enhanced PKCβ-dependent vasoconstrictor reactivity to endothelin-1 in pulmonary arteries from IH rats. In addition, this PKCβ/mitoROS signaling pathway could be stimulated by the PKC activator PMA in pulmonary arteries from control rats, and in both rat and human pulmonary arterial smooth muscle cells. These responses to PMA were attenuated by inhibition of mitoK$_{ATP}$ or PICK1. Subcellular fractionation and proximity ligation assays further demonstrated that PKCβ acutely translocates to mitochondria upon stimulation and associates with PICK1. We conclude that a PKCβ/mitoROS signaling axis contributes to enhanced vasoconstriction and pHTN after IH. Furthermore, PKCβ mediates pulmonary vasoconstriction through interaction with PICK1, activation of mitoK$_{ATP}$, and subsequent mitoROS generation.

Keywords: sleep apnea; pulmonary hypertension; vascular smooth muscle; mitochondria; reactive oxygen species

Intermittent hypoxia (IH) resulting from sleep apnea (SA) is a major cause of morbidity and mortality, affecting an estimated 5–25% of adults (1–3). In addition to causing systemic cardiovascular disease, IH associated with SA is a common cause of group 3 pulmonary hypertension (pHTN, i.e., associated with lung disease/hypoxemia) (1, 4, 5). The presence of pHTN in patients with SA correlates with greater dyspnea, exercise intolerance, and mortality (6). Moreover, SA exacerbates pHTN in patients

(Received in original form October 9, 2019; accepted in final form February 10, 2020)

Supported by U.S. National Institutes of Health grants R01 HL088151 (L.V.G.B.), R01 HL095640 (B.R.W.), R01 HL082799 (N.L.K.), R01 HL111084 (N.L.J.), R01 HL132883, R01 HL088192, T32 HL007736 (T.C.R.), K12-GM-088021 (Principal Investigator: A. Wandinger-Ness), and Institutional Development Award grant by the National Institute of General Medical Sciences (NIGMS) P20GM103451 (J.B.S.), and American Heart Association grants 12POST8690008 (J.B.S.), 13PRE14580015 (C.E.N.), 18AIREA33960020 (J.B.S.), and 16GRNT27700010 (T.C.R.).

Author Contributions: J.B.S. contributed to study conception and design, performed experiments, analyzed and interpreted data, and drafted and revised the manuscript. C.E.N., M.A.S., L.W.-C., S.Y., and L.M.H. performed experiments, analyzed and interpreted data, and revised the manuscript. J.R.S., L.V.G.B., B.R.W., and N.L.K. contributed to study design, interpreted data, and revised the manuscript. N.L.J. contributed to study conception and design, performed experiments, analyzed and interpreted data, and revised the manuscript. T.C.R. contributed to study conception and design, supervised study execution, interpreted data, and revised the manuscript.

Correspondence and requests for reprints should be addressed to Thomas C. Resta, Ph.D., Department of Cell Biology and Physiology, University of New Mexico Health Sciences Center, MSC 08-4750, 1 University of New Mexico, Albuquerque, NM 87131-0001. E-mail: tresta@salud.unm.edu.

This article has a data supplement, which is accessible from this issue's table of contents at www.atsjournals.org.

Am J Respir Cell Mol Biol Vol 62, Iss 6, pp 732–746, Jun 2020

Originally Published in Press as DOI: 10.1165/rcmb.2019-0351OC on February 12, 2020
Internet address: www.atsjournals.org

with comorbid conditions (overlap syndrome), including chronic obstructive pulmonary disease, diastolic heart failure, obesity hypoventilation syndrome, restrictive lung disease, and residence at high altitude (2, 7–9).

Despite the increasing recognition and clinical impact of this disorder, the cardiovascular sequelae of SA-induced pHTN have gone largely unexplored. Our laboratory and others have begun to investigate the mechanisms of pHTN using animal models of SA involving exposure to IH, which is considered to be the primary contributing factor to the pathogenesis of SA (10–12). These mechanisms of pHTN include oxidative stress, vasoconstriction, and arterial remodeling (4, 10–15). Furthermore, IH augments pulmonary vasoconstrictor reactivity through a PKC-dependent (but Rho kinase–independent) Ca^{2+}-sensitization pathway in pulmonary arterial smooth muscle cells (PASMCs) (14) that is distinct from those associated with other forms of pHTN (16–21). Interestingly, this pathway is mediated by PKCβ, a PKC isoform that has not previously been linked to vasoconstriction (14), and is coupled to endothelin receptor stimulation only after IH exposure. However, neither the signaling mechanisms by which PKCβ mediates PASMC contraction nor the contribution of this pathway to the development of IH-induced pHTN is understood.

Mitochondrial dysfunction has been implicated as an important consequence of PKCβ signaling in several disease states (22, 23). Considering the involvement of PKCβ (14) and reactive oxygen species (ROS) (12) in IH-induced pHTN, and the importance of oxidative stress and mitochondrial dysfunction in SA syndrome (24), we hypothesized that PKCβ-induced mitochondrial ROS (mitoROS) signaling augments pulmonary vasoconstrictor reactivity after IH and contributes to the development of IH-induced pHTN.

An additional goal of this study was to define the signaling mechanism by which PKCβ causes pulmonary vasoconstriction. A potential mediator of this response is PICK1 (protein interacting with C kinase 1), a scaffolding and membrane-anchoring protein that interacts directly with a variety of membrane proteins to regulate their activity and signaling (25). PICK1 additionally targets other PKC isoforms to the mitochondria in a ligand-specific manner (26, 27). However, whether PICK1 protein interacts with PKCβ to facilitate mitoROS generation has not previously been addressed.

A possible target of PKCβ to regulate mitochondrial function is the mitochondrial ATP-sensitive K^+ ($mitoK_{ATP}$) channel. This channel is structurally and pharmacologically distinct from sarcolemmal K_{ATP} channels (28) and is located on the mitochondrial inner membrane. When activated, these channels mediate K^+ influx, mitochondrial membrane potential ($\Delta\Psi_M$) depolarization, and matrix alkalinization (29) that increases O_2^- generation by the electron transport chain (ETC) (30). Therefore, we further hypothesized that PKCβ mediates pulmonary vasoconstriction through a novel signaling mechanism involving interaction with PICK1, activation of $mitoK_{ATP}$ channels, and subsequent mitoROS generation. To test these hypotheses, protocols employed both pharmacologic and genetic approaches, along with a variety of experimental preparations from single cell (human, rodent) imaging to video-microscopy of pressurized small pulmonary arteries from control and IH rats. We also assessed the significance of PKCβ and mitoROS in the development of IH-induced pHTN in whole-animal studies.

Methods

All protocols and surgical procedures were approved by the Institutional Animal Care and Use Committee of the University of New Mexico Health Sciences Center (Albuquerque, NM). Male rats were selected for the present study because male sex is an important risk factor for obstructive SA (31). Age-matched male Wistar rats (~250–350 g; age 3–4 mo; Harlan Industries) were exposed to either IH with CO_2 supplementation (3-min cycles of 5% O_2, 5% CO_2/air flush) or sham (air-air) conditions (7 h/d, 4 wk) as described previously (14, 15). This model of SA reproduces both the pHTN and systemic hypertension that is characteristic of human SA (14, 15, 32). Additional animals were housed under normal (control) room air conditions for studies involving pharmacologic stimulation of PKC signaling.

An expanded METHODS section detailing the protocols and statistics used is available in the data supplement.

Results

Involvement of ROS and PKCβ in IH-induced pHTN

We determined the contribution of ROS and PKCβ to the development of IH-induced pHTN by measuring indices of pHTN in rats after chronic oral administration of the superoxide dismutase mimetic Tempol (1 mM in drinking water [33]), the selective PKCβ inhibitor LY-333531 (14, 34) (20 mg/kg/d [35]; in Bio-Serv dough pills), or their respective vehicles during the entire 4-week period of IH or sham exposure.

IH exposure in vehicle-treated rats resulted in greater right ventricular systolic pressure (RVSP) compared with sham-treated animals (Figures 1A–1D), indicative of pHTN. This effect of IH was abolished in rats treated with either Tempol or LY-333531. Heart rates did not differ between groups or treatments (Table E1 in the data supplement). In addition, cardiac contractility was not altered by IH (sham, 72.00 ± 6.38; IH, 65.10 ± 3.58), Tempol (IH vehicle, 62.46 ± 6.42; IH Tempol, 69.28 ± 7.66), or LY-333531 (IH vehicle, 67.75 ± 3.45; IH LY-333531, 85.99 ± 13.67) (all values in 1/s).

Exposure to IH also increased the ratios of right ventricle/total ventricle weight and right ventricle/left ventricle plus septum (LV+S) weight (Tables E2 and E3), demonstrating RV hypertrophy. Consistent with the effects of O_2^- scavenging and PKCβ inhibition on RVSP, treatment with either Tempol or LY-333531 prevented IH-induced RV hypertrophy. Tempol had no effect on the ratios of (LV+S)/body weight in either group. Although LY-333531 did not alter (LV+S)/body weight in sham-treated rats, this ratio was slightly (but significantly) greater in IH rats treated with LY-333531 than in those treated with vehicle. Body weights were unaltered by administration of Tempol or LY-333531 in either sham or IH rats (Tables E2 and E3). Collectively, these data support the involvement of both O_2^- and PKCβ in IH-induced pHTN.

IH Increases Basal and Endothelin-1–induced Pulmonary Arterial O_2^- Levels and Augments Vasoconstrictor Reactivity through PKC/MitoROS Signaling

We have previously demonstrated that IH augments endothelin-1 (ET-1)–dependent

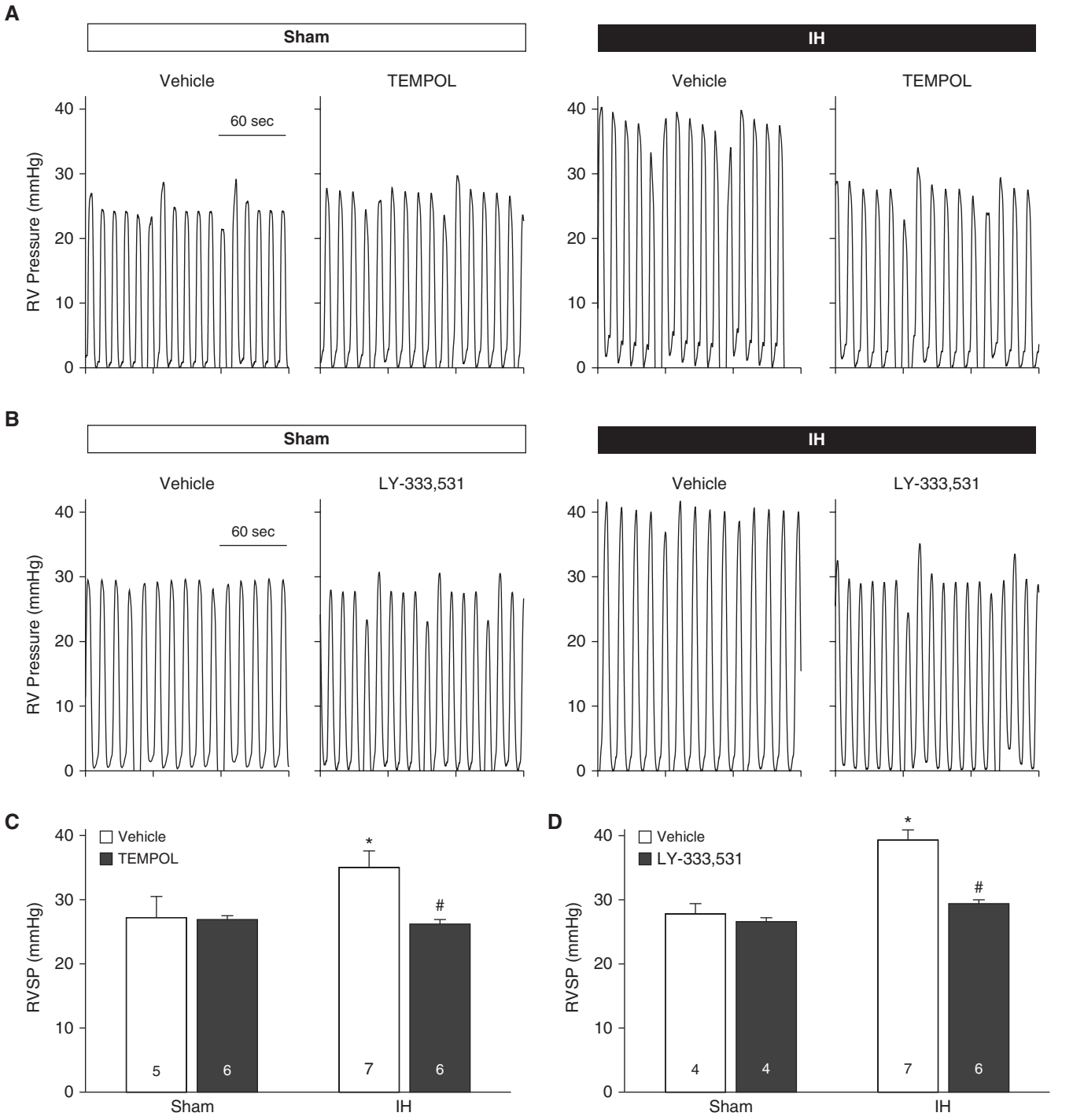

Figure 1. Evidence for involvement of O_2^- and PKCβ in intermittent hypoxia (IH)-induced pulmonary hypertension. (*A* and *B*) Sample traces of right ventricular (RV) pressure in isoflurane-anesthetized sham and IH rats treated with the reactive oxygen species scavenger Tempol (1 mM in drinking water) (*A*), the selective PKCβ inhibitor LY-333531 (20 mg/kg/d, orally), or their respective vehicles during the entire 4-week exposure period (*B*). (*C* and *D*) RV systolic pressure (RVSP) in sham and IH rats treated with Tempol (*C*), LY-333531 (*D*), or vehicle. All measurements were performed the day after the 4-week IH or sham protocol. Numbers of animals are indicated in bars. $^*P < 0.05$ versus sham vehicle. $^\#P < 0.05$ versus IH vehicle. Analyzed by two-way ANOVA and Student-Newman-Keuls test.

pulmonary vasoconstrictor reactivity through PKCβ-mediated PASMC Ca^{2+}-sensitization (14). We used ET-1 as a vasoconstrictor stimulus because it is a potent endogenous vasoconstrictor that has been implicated in pHTN (36). We assessed the contribution of ROS to ET-1–induced vasoconstriction in endothelium-disrupted, pressurized pulmonary arteries (⩾50 μm inner diameter) using a preparation that permits fluorescence detection of O_2^- using dihydroethidium (DHE) (13, 18) and

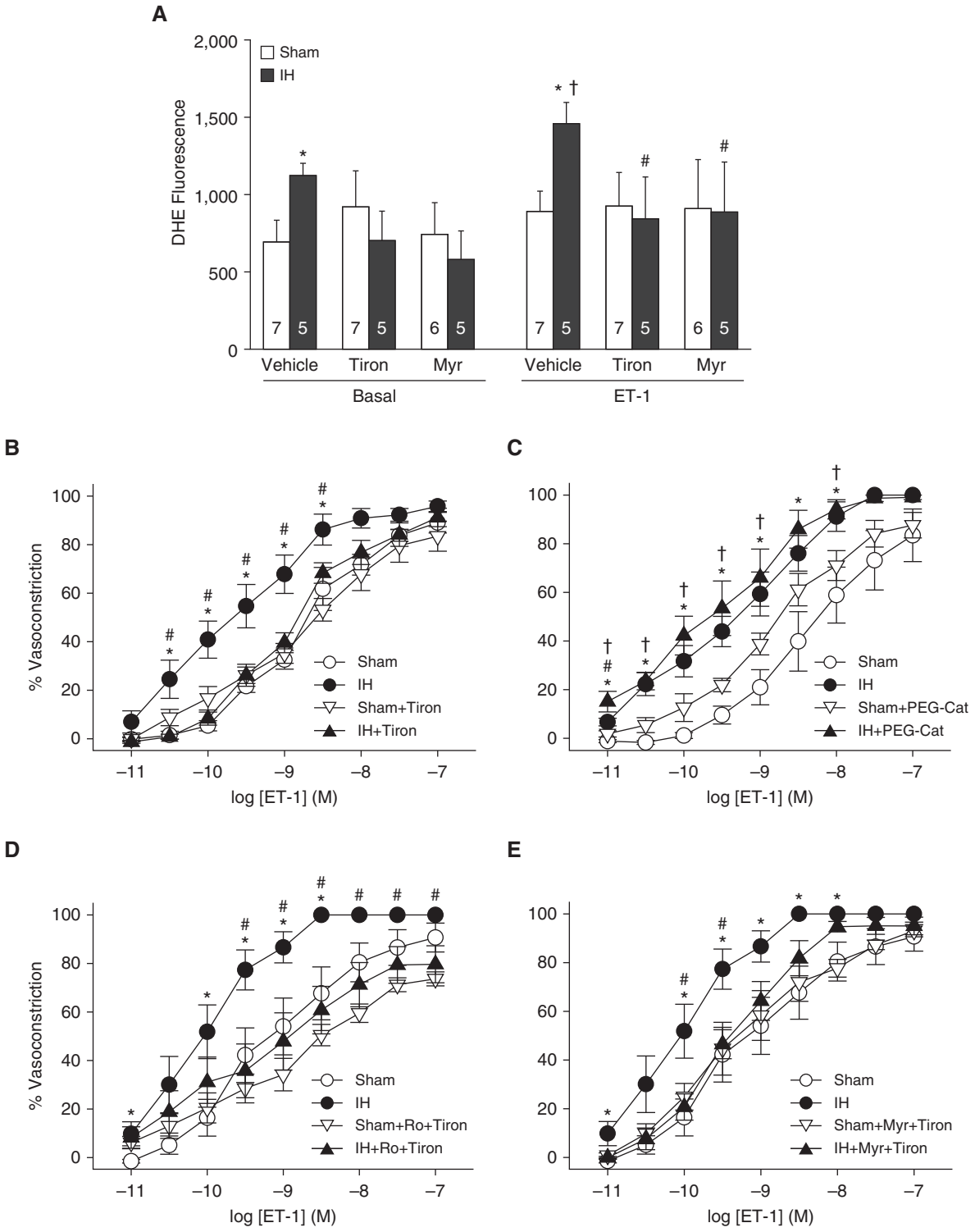

Figure 2. IH increases basal and endothelin-1 (ET-1)–induced O_2^- levels in pulmonary arteries through PKCα/β, leading to enhanced vasoconstrictor sensitivity. (*A*) Basal and ET-1 (1 nmol/L)–stimulated dihydroethidium (DHE) fluorescence (mean background-subtracted fluorescence intensity) in endothelium-disrupted, pressurized pulmonary arteries from sham and IH rats. Experiments were conducted in the presence of the O_2^- scavenger tiron (10 mmol/L), the selective PKCα/β inhibitor myr-PKC (10 μmol/L), or vehicle. Numbers of animals are indicated in bars. $^*P < 0.05$ versus sham vehicle. $^\#P < 0.05$ versus ET-1 IH vehicle. $^\dagger P < 0.05$ versus basal IH vehicle. (*B–E*) Vasoconstrictor responses (percent baseline inner diameter) to ET-1 (10^{-11} to 10^{-7} mol/L) in endothelium-disrupted, pressurized pulmonary arteries from sham and IH rats in the presence of tiron (10 mmol/L) (*B*), polyethylene glycol–catalase (PEG-Cat; 250 U/ml) (*C*), the general PKC antagonist Ro 31-8220 (5 μmol/L) + tiron (*D*), myr-PKC (10 μmol/L) + tiron, or their respective vehicles (*E*). $n = 4$–9 rats/treatment. $^*P < 0.05$ IH vehicle versus sham vehicle. $^\#P < 0.05$ IH drug versus IH + vehicle. $^\dagger P < 0.05$ IH + drug versus sham + drug. (*A–E*) Analyzed by two-way repeated-measures ANOVA (*A*) or two-way ANOVA (*B–E*) followed by the Student-Newman-Keuls test. myr = myristolated; Ro = Ro 31-8220.

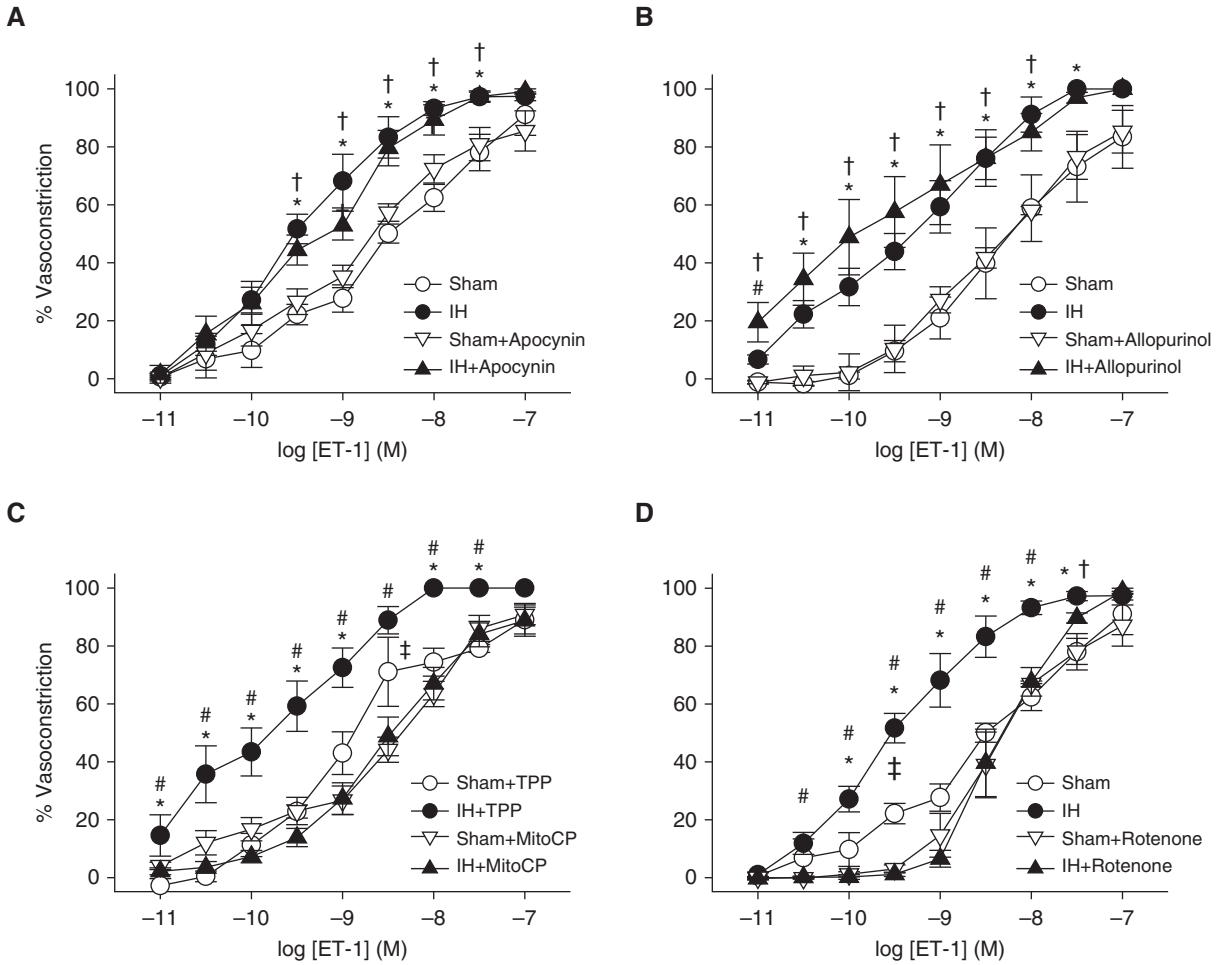

Figure 3. Mitochondrial reactive oxygen species mediate enhanced pulmonary vasoconstrictor sensitivity to ET-1 after IH. (*A–D*) Vasoconstrictor responses (percent baseline inner diameter) to ET-1 (10^{-11} to 10^{-7} mol/L) in endothelium-disrupted, pressurized pulmonary arteries from sham and IH rats in the presence of the non-selective NADPH oxidase inhibitor apocynin (30 μmol/L) (*A*), the xanthine oxidase inhibitor allopurinol (100 μmol/L) (*B*), the mitochondria-targeted antioxidant mito-carboxy proxyl (MitoCP; 0.5 μmol/L) or triphenylphosphonium (TPP; negative control, 0.5 μmol/L) (*C*), the mitochondrial complex I inhibitor rotenone (10 μmol/L), or their respective vehicles (*D*). $n = 4$–5 rats/treatment. $^{*}P < 0.05$ IH vehicle versus sham vehicle. $^{\#}P < 0.05$ IH drug versus IH vehicle. $^{\dagger}P < 0.05$ IH drug versus sham drug. $^{\ddagger}P < 0.05$ sham drug versus sham vehicle. Analyzed by two-way ANOVA followed by the Student-Newman-Keuls test.

video-microscopic measurements of vessel inner diameter. IH increased both basal and ET-1–stimulated DHE fluorescence (Figure 2A), and these responses were prevented by the O_2^- scavenger tiron (37). However, DHE fluorescence was unaltered by ET-1 in arteries from sham-treated rats. We have previously documented the specificity of DHE for detection of O_2^- in this preparation as well as similar ones (33, 38).

In agreement with these observations, tiron prevented increased vasoconstriction to ET-1 in arteries from IH rats without altering responses in the sham group (Figure 2B). In contrast, effects of IH to increase ET-1 responses persisted in the presence of the membrane-permeable H_2O_2 scavenger polyethylene glycol-catalase (33) (Figure 2C). These findings indicate that O_2^-, rather than H_2O_2, mediates augmented vasoconstrictor reactivity to ET-1 after IH.

To determine whether PKCβ signals proximal or distal to the site of agonist-induced O_2^- generation in IH arteries, we evaluated basal and ET-1–stimulated DHE fluorescence after PKCβ inhibition with the PKCα/β inhibitor myr-PKC (14). We have previously demonstrated that myr-PKC prevents enhanced vasoconstrictor sensitivity to ET-1 after IH, similar to the effects of LY-333531 (14). Interestingly, myr-PKC prevented both the enhanced basal and ET-1–induced O_2^- generation in vessels from IH rats (Figure 2A). Consistent with PKCβ and O_2^- signaling in a common pathway, combined ROS scavenging and PKC inhibition (with either the general PKC inhibitor Ro 31-8330 or myr-PKC) attenuated vasoconstrictor responses to ET-1 in vessels from IH-exposed, but not sham-treated, rats and normalized responses between groups (Figures 2D and 2E), similar to the effects of tiron (Figure 2B) or PKC inhibition (14) alone. Together, these findings suggest that PKCβ is required for enhanced basal and ET-1–induced pulmonary arterial O_2^- production after IH, and that PKCβ and O_2^- signal in series to mediate enhanced vasoconstrictor sensitivity in this setting.

We next examined potential sources of O_2^- mediating elevated vasoconstrictor reactivity to ET-1, including NADPH oxidase (NOX), xanthine oxidase, and mitochondria. Whereas greater reactivity to ET-1 after IH persisted after inhibition of NOX with apocynin (37) (Figure 3A), or xanthine oxidase with allopurinol (Figure 3B), the mitoROS scavenger mitocarboxy proxyl (MitoCP) (39) abolished this effect of IH while having minimal effects in the sham group (Figure 3C). Because MitoCP is a conjugate of triphenylphosphonium, a lipophilic cation group that targets this compound to the mitochondria by virtue of the transmembrane potential (40), we used triphenylphosphonium as a negative control in these experiments. To further evaluate the mitochondrial ETC as a potential source of O_2^- in this response, we repeated these experiments in the presence of the mitochondrial complex I inhibitor rotenone (41) or vehicle. Rotenone, which inhibits the ETC proximal to the site of O_2^- production (41), markedly attenuated vasoconstrictor reactivity to ET-1 in IH vessels while having little effect in sham arteries, and normalized responses between groups. The similar inhibitory effects of MitoCP and rotenone therefore establish mitochondria as a primary source of O_2^- mediating augmented vasoconstrictor reactivity after IH.

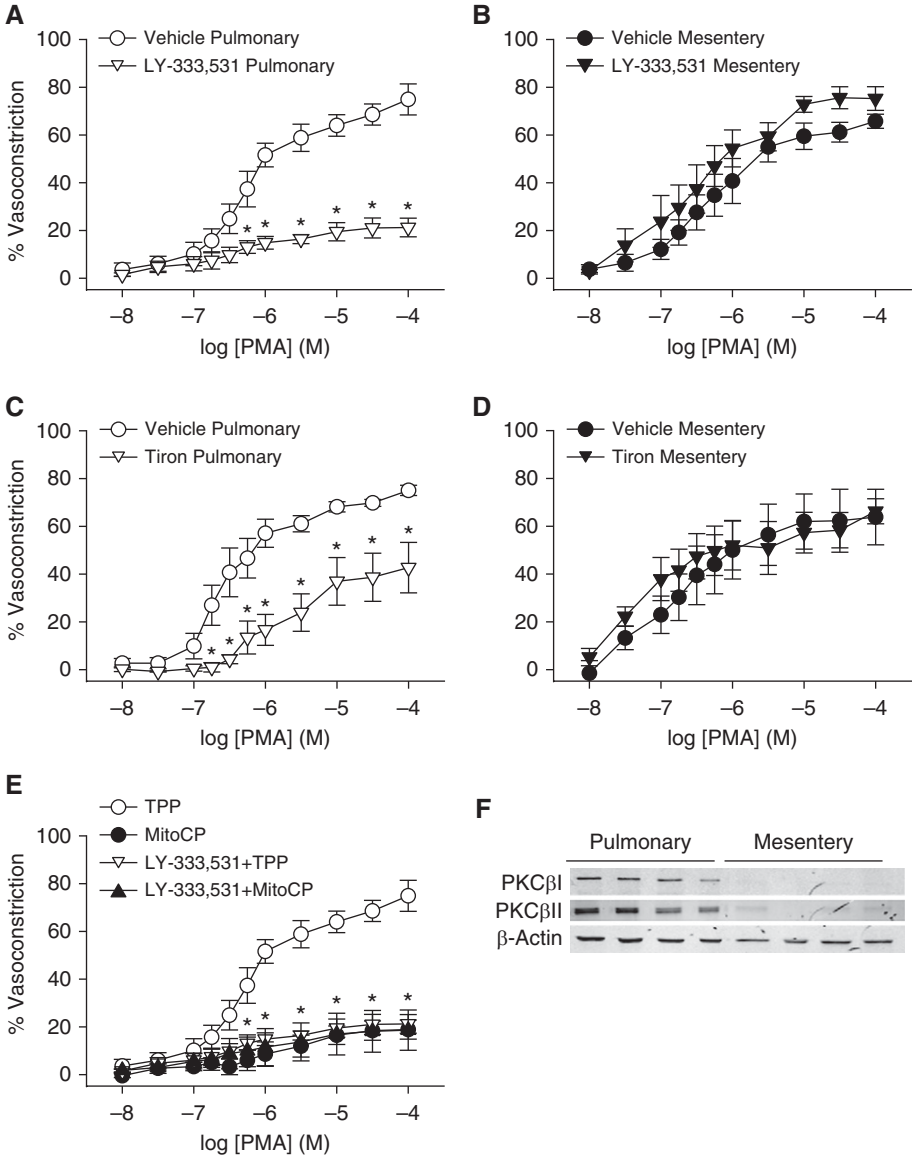

Figure 4. PKCβ and mitochondrial reactive oxygen species contribute to PMA-induced constriction of pulmonary, but not mesenteric, arteries—a response associated with greater PKCβ expression in pulmonary arteries. (*A–D*) Vasoconstrictor responses (percent baseline inner diameter) to the PKC agonist PMA (10^{-8} to 10^{-4} mol/L) in endothelium-disrupted, pressurized pulmonary (*A* and *C*) and mesenteric arteries (*B* and *D*) from control rats in the presence of the PKCβ inhibitor LY-333531 (10 nmol/L) (*A* and *B*) or the O_2^- scavenger tiron (10 mmol/L) (*C* and *D*). (*E*) Reactivity to PMA in pulmonary arteries from control rats in the presence of the mitochondria-targeted antioxidant MitoCP (0.5 μmol/L), TPP (negative control, 0.5 μmol/L), or in the combined presence of the PKCβ inhibitor LY-333531 or vehicle. Data in *A* are reproduced in *E* for illustrative purposes. (*F*) Western blots for PKCβI, PKCβII, and β-actin in intrapulmonary and mesenteric arteries. $n = 4$–5 rats/treatment or group. (*A*, *C*, and *E*) $^*P < 0.05$ versus vehicle (*A* and *C*), or all treatments versus TPP (*E*). (*A–E*) Analyzed by unpaired *t* test (*A–D*) or two-way ANOVA followed by the Student-Newman-Keuls test (*E*). Readers may view the uncut gels for *F* in the data supplement.

MitoROS Mediate PKCβ-Dependent Constriction of Pulmonary, but Not Mesenteric, Arteries

Although PKCβ-mediated myofilament Ca^{2+}-sensitization and resultant pulmonary vasoconstriction are coupled to receptor stimulation only after IH exposure (14), we questioned whether an intact PKCβ-O_2^- signaling axis is present in pulmonary arteries from normoxic rats, and can be stimulated pharmacologically to allow a better mechanistic analysis of this pathway. We also studied small mesenteric arteries to determine whether PKCβ-dependent vasoconstriction is a global phenomenon that occurs in both pulmonary and systemic circulations. To explore these possibilities, we assessed the effects of PKCβ inhibition or ROS scavenging on vasoconstrictor and vessel wall $[Ca^{2+}]_i$ (14, 33, 37) responses to the PKC agonist PMA in pressurized, endothelium-disrupted pulmonary and mesenteric arteries from control animals. In contrast to the robust vessel wall $[Ca^{2+}]_i$ response associated with vasoconstriction to depolarizing concentrations of KCl in both pulmonary (Figures E1A and E1B) and mesenteric arteries (Figures E1C and E1D), PMA caused vasoconstriction independently of a change in vessel wall $[Ca^{2+}]_i$ in both vessel types (Figures E1E and E1F), demonstrating the importance of myofilament Ca^{2+}-sensitization to these

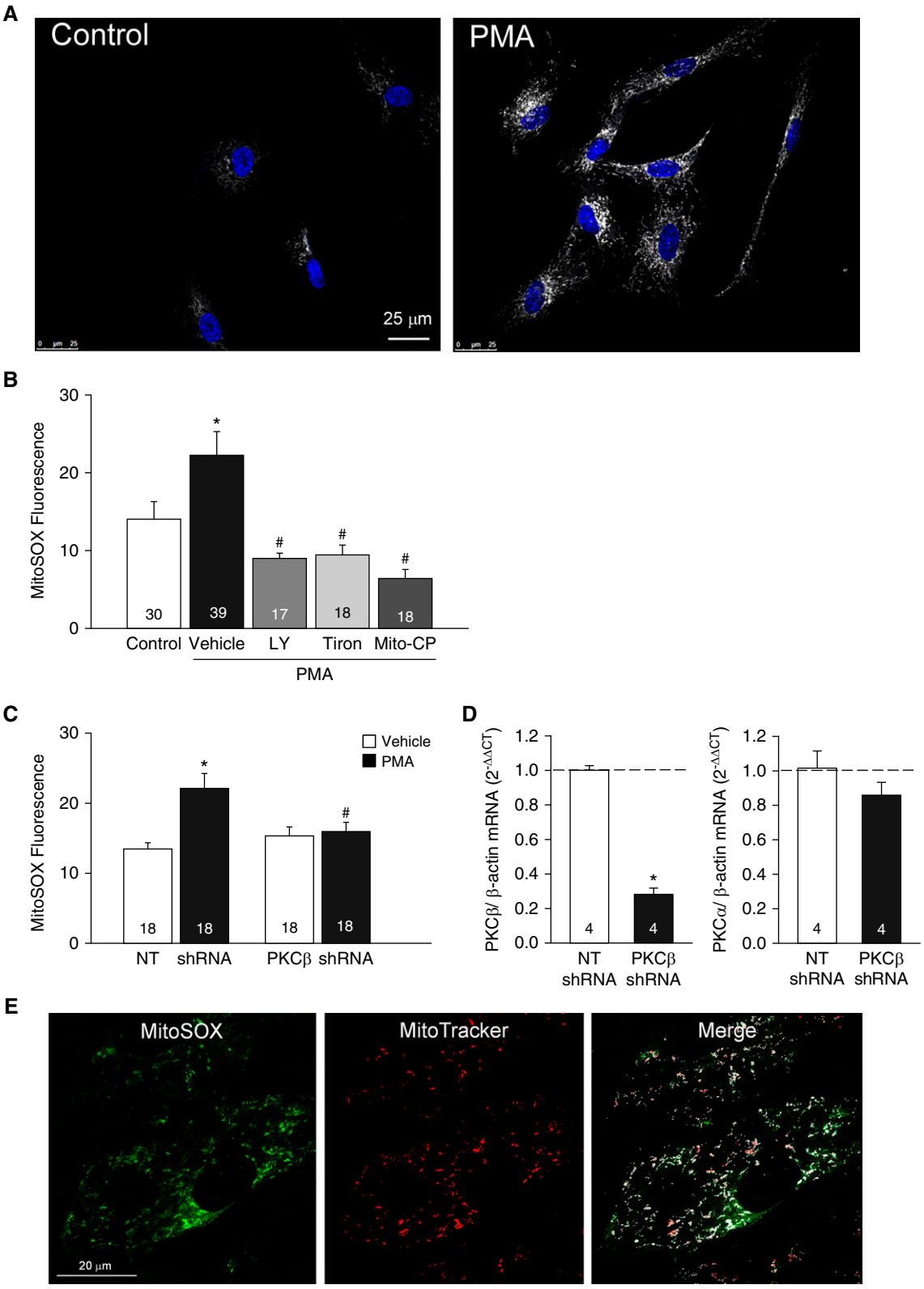

Figure 5. PKCβ induces mitochondrial O_2^- generation in human and rat pulmonary arterial smooth muscle cells (PASMCs). (*A*) MitoSOX (white) and nuclear staining (blue) in human PASMCs treated with the PKC agonist PMA (1 μmol/L) or vehicle (control). Scale bar: 25 μm. (*B*) MitoSOX fluorescence (mean background-subtracted fluorescence intensity) ± PMA (1 μmol/L) in the presence of the PKCβ inhibitor LY-333531 (LY, 10 nmol/L), the O_2^- scavenger tiron (10 mmol/L), the mitochondrial antioxidant Mito-CP (0.5 μmol/L), or vehicle in human PASMCs. $n = 17–39$ images (specified in bars) from

responses. PKCβ inhibition with LY-333531 markedly attenuated vasoconstriction to PMA in pulmonary arteries (Figure 4A), supporting a dominant role for PKCβ in PMA-dependent constriction. In contrast, PMA-dependent vasoconstriction of mesenteric arteries was unaltered by PKCβ inhibition (Figure 4B), consistent with dramatically lower expression of PKCβ splice variants (PKCβI and βII) than in pulmonary arteries (Figure 4F).

We next examined whether PKCβ stimulation in pulmonary arteries from control rats mediates constriction through a mitoROS-dependent mechanism similar to that observed with ET-1 in vessels from IH rats. Similar to the effects of PKCβ inhibition, tiron attenuated PMA-induced constriction of pulmonary arteries (Figure 4C), but not mesenteric arteries (Figure 4D). MitoCP also greatly inhibited constrictor responses to PMA in control pulmonary arteries (Figure 4E). Furthermore, the inhibitory effects of LY-333531 and MitoCP were not additive, consistent with PKCβ and mitoROS signaling in a common pathway to mediate pulmonary vasoconstriction.

PKCβ Increases MitoROS Levels in PASMCs

In agreement with functional studies in whole arteries (Figures 3 and 4), we found that PMA stimulated mitoROS production in both human PASMCs (Figures 5A and 5B) and primary cultures of rat PASMCs (Figure 5C), as assessed using the mitochondria-targeted fluorescent O_2^- indicator MitoSOX. This response occurred within 1 minute of PMA exposure (Figures 5A and 5B) and persisted at 4 hours (MitoSOX fluorescence [AU]: 11.8 ± 0.6 in vehicle vs. 19.1 ± 1.2 in PMA [1 μmol/L]-treated cells; $P < 0.05$). Furthermore, PMA-induced mitoROS production was prevented by LY-333531, tiron, and MitoCP (Figure 5B), as well as knockdown of PKCβ using shRNA (Figure 5C), demonstrating the specific role of PKCβ in mediating this response. Quantitative PCR verified that PKCβ shRNA decreased PKCβ, but not PKCα, mRNA expression (Figure 5D). Localization of MitoSOX to mitochondria was confirmed by colocalization with MitoTracker Deep Red (Figure 5E).

PICK1 Facilitates Mitochondrial O_2^- Generation and PKC-mediated Pulmonary Vasoconstriction, and Demonstrates Increased Colocalization with PKCβII in Response to PMA

PICK1 is a scaffolding protein that organizes the subcellular localization of a variety of proteins, including PKCα (27). We have previously demonstrated that PICK1 is expressed in rat PASMCs, where it regulates the activity of acid-sensing ion channel 1 (25). To test the hypothesis that PICK1 interacts with PKCβ and facilitates PKCβ-dependent vasoconstriction and mitoROS production, we measured vasoconstrictor responses to PMA after administration of the competitive PICK1 inhibitor FSC231 (26) in both pulmonary and mesenteric arteries. Similar to the effects of LY-333531 and MitoCP (Figures 4A and 4E), FSC231 largely attenuated constriction to PMA in pulmonary arteries (Figure 6A) but had no effect in mesenteric arteries (Figure 6B). PICK1 inhibition also prevented PMA-induced mitoROS generation in rat PASMCs (Figures 6C and 6D) in a manner analogous to that of PKCβ inhibition with LY-333531 or shRNA (Figures 5B and 5E).

Duolink proximity ligation assays (PLAs) further demonstrated the physical association of PICK1 and PKCβI/II in rat PASMCs (indicated by red puncta in Figures 6E and 6G). This assay uses *in situ* PLA probes (secondary antibodies conjugated to DNA), allowing oligonucleotide amplification between proteins <40 nm in proximity (25). Negative control experiments were conducted in the presence of each primary antibody alone or with both primary antibodies omitted (Figure 6I). Interestingly, stimulation of PKCβ with PMA increased the association of PICK1 with PKCβII (Figures 6G and 6H), but not with PKCβI (Figures 6E and 6F). Collectively, these data support an effect of PICK1 to facilitate PKCβII-induced mitoROS generation and vasoconstriction.

PKCβ Translocates to Mitochondria after Stimulation in PASMCs

Immunofluorescence microscopy in human PASMCs revealed distinct colocalization of both PKCβI and PKCβII with the mitochondrial marker MitoTracker Deep Red (Figure 7A). Western blotting of subcellular fractions of rat PASMC cultures revealed that PKCβI and PKCβII were preferentially localized to the cytosolic fraction under basal conditions, but underwent acute trafficking to mitochondria upon stimulation with PMA (Figures 7B and 7C). PICK1 inhibition with FSC231 had no effect on this response, suggesting that PICK1 mediates PKCβ-induced mitoROS production through mechanisms that are independent of trafficking PKCβ to mitochondria.

Role of Mitochondrial K_{ATP} Channels in PKC-induced Mitochondrial Membrane Potential ($\Delta\Psi_M$) Depolarization, MitoROS Production, and Pulmonary Arterial Constriction

Considering the importance of mitoK_{ATP} channels in the regulation of $\Delta\Psi_M$ and mitoROS generation (30), we next examined their contribution to PMA-induced pulmonary arterial constriction and mitoROS production. The specific mitoK_{ATP} channel antagonist 5-hydroxydecanoate (5-HD) (42, 43) attenuated constriction to both PMA (Figure 8A) and the selective mitoK_{ATP} channel activator diazoxide (42, 43) (Figure 8B) in pressurized rat pulmonary arteries, without altering vessel wall $[Ca^{2+}]_i$ (not shown). In agreement with findings from isolated vessels, 5-HD prevented both PMA- and diazoxide-induced increases in

Figure 5. (*Continued*). three experiments/treatment. *$P < 0.05$ versus control. #$P < 0.05$ versus PMA + vehicle. (*C*) PKCβ shRNA prevents PMA (10 μmol/L)-induced increases in MitoSOX fluorescence in primary cultures of rat PASMCs. $n = 20$ images from four experiments (rats)/treatment. (*D*) shRNA knockdown of PKCβ mRNA in primary cultures of rat PASMCs (left graph). PKCβ shRNA transfection has no effect on PKCα mRNA expression (right graph). $n = 4$ rats/treatment. *$P < 0.05$ versus nontargeting (NT) shRNA. (*E*) Colocalization of MitoSOX and MitoTracker Deep Red in primary cultures of rat PASMCs (green, MitoSOX; red, MitoTracker; white, colocalization in merged image). Scale bar: 20 μm. *$P < 0.05$ versus vehicle NT shRNA. #$P < 0.05$ versus PMA NT shRNA. (*B–D*) Analyzed by one-way ANOVA (*B*), two-way ANOVA (*C*), or unpaired *t* test (*D*). *Post hoc* comparisons were made using the Student-Newman-Keuls test.

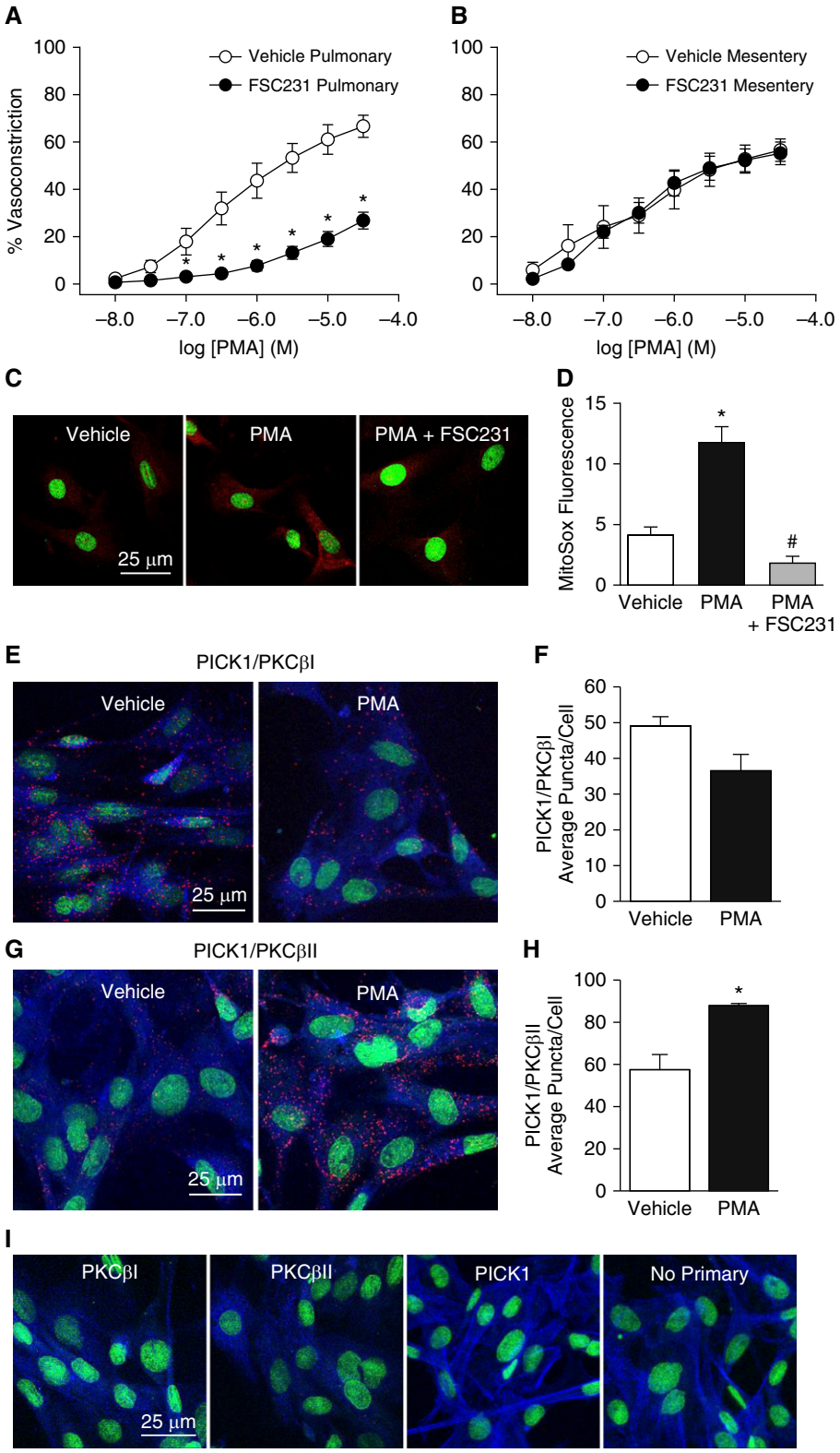

Figure 6. PICK1 (protein interacting with C kinase 1) facilitates mitochondrial O_2^- generation and PKC-mediated pulmonary vasoconstriction, and demonstrates increased colocalization with PKCβII in response to PMA. (*A* and *B*) Vasoconstrictor responses to the PKC agonist PMA (10^{-8} to 3×10^{-5} mol/L) in endothelium-disrupted, pressurized pulmonary (*A*) and mesenteric arteries (*B*) from control rats in the presence of the PICK1 inhibitor FSC231 (50 μmol/L) or vehicle. $n = 5$ rats/treatment.

MitoSOX fluorescence in human PASMCs (Figures 8C and 8D), implicating mitoK$_{ATP}$ channels in both PKC-dependent mitoROS generation and vasoconstriction.

We further evaluated the ability of PKC to stimulate mitoK$_{ATP}$ channels by assessing mitoK$_{ATP}$ channel-dependent $\Delta\Psi_M$ depolarization in live-cell and vessel imaging experiments using the mitochondria-targeted, cationic, fluorescent potentiometric indicator tetramethylrhodamine methyl ester perchlorate (TMRM) (44). This probe accumulates in the mitochondrial matrix as a result of the large negative $\Delta\Psi_M$, and thus fluorescence intensity decreases with $\Delta\Psi_M$ depolarization (45). Mitochondrial localization of TMRM was confirmed by colocalization with MitoTracker Deep Red (Figure 8E). Consistent with the effects of PKC to increase mitoROS production through activation of mitoK$_{ATP}$ channels (Figures 8C and 8D), PMA and diazoxide caused $\Delta\Psi_M$ depolarization in both human PASMCs (Figures 8F and 8G) and pressurized rat pulmonary arteries (Figure 8H). Furthermore, these responses were blocked by 5-HD, demonstrating their dependency on mitoK$_{ATP}$ channel activation. The protonophore carbonyl cyanide 3-chlorophenylhydrazone was used as a positive control to induce $\Delta\Psi_M$ depolarization, resulting in a decrease in TMRM fluorescence in both human PASMCs ($-62.0 \pm 9.3\%$ at time = 12 min) and isolated arteries (Figure 8H).

Discussion

The overall objective of this study was to identify signaling mechanisms responsible for PKCβ-mediated pulmonary vasoconstriction, and the role of this signaling pathway in IH-dependent increases in vasoconstrictor reactivity and pHTN in a clinically relevant rat model of SA. The major findings from this study are that: *1*) PKCβ and oxidant signaling accounts for IH-induced increases in RVSP and RV hypertrophy; *2*) mitoROS mediate enhanced PKCβ-dependent vasoconstrictor reactivity to ET-1 in pressurized small pulmonary arteries from IH rats; *3*) although this PKCβ/mitoROS pathway is coupled to endothelin receptor stimulation only after IH, this signaling mechanism is intact in pulmonary arteries (but not mesenteric arteries) from control rats, and

in both rat and human PASMCs, and can be stimulated pharmacologically by PMA; *4*) PKCβ acutely translocates to mitochondria upon stimulation and colocalizes with the scaffolding protein PICK1; and *5*) mitoK$_{ATP}$ channels and PICK1 contribute to PKCβ-dependent mitoROS production and pulmonary vasoconstriction. Collectively, these studies support a major role for PKCβ/mitoROS signaling in the enhanced pulmonary vasoconstrictor sensitivity and pHTN responses to IH. Furthermore, PKCβ mediates pulmonary vasoconstriction through a previously undescribed mechanism involving mitochondrial translocation, interaction with the scaffolding protein PICK1, activation of mitoK$_{ATP}$ channels, and mitoROS generation.

IH and pHTN

Whereas mechanisms of pHTN associated with chronic sustained hypoxia have been extensively studied, relatively little is known regarding the effects of IH on the pulmonary circulation. However, we previously reported that whereas long-term IH exposure in rats has minimal effects to cause arterial remodeling, IH leads to augmented pulmonary vasoconstrictor reactivity to receptor agonists, including the thromboxane analog U-46619 (15) and ET-1 (14). Furthermore, IH enhances vasoconstrictor reactivity to ET-1 in small pulmonary arteries through an increase in PASMC Ca^{2+} sensitivity or Ca^{2+}-independent contractile mechanisms (14). In contrast, responses to depolarizing concentrations of KCl are unaltered by IH (14), suggesting that IH does not increase basal Ca^{2+} sensitivity, but rather promotes coupling of receptor stimulation to PASMC contraction. This effect of IH was prevented by selective inhibition of PKCβ, but not Rho kinase (14). Interestingly, this mechanism of increased PKCβ-dependent arterial constriction after IH stands in contrast to our findings of enhanced Rho kinase–mediated Ca^{2+}-sensitization resulting from chronic hypoxia (18). Furthermore, IH has no effect on either arterial PKCβ mRNA or protein levels (14), suggesting that greater vasoconstrictor reactivity after IH is not dependent on changes in PKCβ gene or protein expression. Rather, exposure to IH selectively links membrane receptor stimulation to PKCβ-mediated pulmonary vasoconstriction, a coupling mechanism that is not present in arteries from control animals.

Role of ROS in IH-induced pHTN

Endogenous ROS, including O_2^- and H_2O_2, are physiologically important intracellular second messengers that are integrally involved in regulation of vascular smooth muscle cell phenotype and contractility. ROS also play a critical role in mediating enhanced vasoconstrictor reactivity (18, 21, 33, 37, 46) and associated pHTN in animal models (33, 47). Similar to our previous observations in the pulmonary circulation of rats exposed to chronic hypoxia (18, 21, 37), our current findings demonstrate an effect of IH to increase both basal and ET-1–stimulated O_2^- levels in small pulmonary arteries, and support a primary contribution of O_2^-, rather than H_2O_2, to enhanced ET-1–dependent vasoconstriction after IH. The lack of a role for H_2O_2 is consistent with evidence that exogenous O_2^- constricts pulmonary arteries independently of H_2O_2 (48). The physiological importance of O_2^- in IH-induced pHTN is further supported by our present findings that chronic administration of the superoxide dismutase mimetic Tempol prevented IH-induced increases RVSP and RV hypertrophy.

NOX (12, 21, 37, 46, 49) and xanthine oxidase (50) are the major sources of ROS implicated in the development of pHTN. However, our current observations indicate that neither inhibition of NOX1/2 with apocynin nor inhibition of xanthine oxidase with allopurinol altered constriction to ET-1 in arteries from IH rats, arguing against a role for these enzymes in altered vasoreactivity after IH. In contrast to these findings, however, mice deficient in the NOX2 subunit gp91phox are protected from IH-induced RV hypertrophy and arterial remodeling (12). Whether this discrepancy is explained by a difference in species or a role for NOX2 that is independent of IH-induced alterations in vasoreactivity is not clear. Although apocynin has been reported to have antioxidant properties that are independent of NOX inhibition (51), such effects are likely minimal at the concentration used in the present study. Supporting this assertion are our findings that apocynin did not attenuate vasoconstriction in vessels from IH rats, whereas the ROS scavengers tiron and polyethylene glycol-catalase produced marked inhibition.

Mitochondria represent an alternative source of ROS that mediate greater vasoconstrictor sensitivity after IH. The mitochondrial ETC includes four protein complexes located in the mitochondrial inner membrane, and is an important source of ROS that mediate responses to both hypoxia (41, 52, 53) and ischemia-reperfusion (45). Complex III is often the principal site of O_2^- generation by the ETC (41, 52), and can produce O_2^- toward the intermembrane space (54), where it may exit the mitochondria to mediate cytosolic signaling or oxidative damage (45). Supporting a role for mitoROS in augmented pulmonary vasoconstrictor reactivity after IH, this response was abolished by the mitochondria-targeted antioxidant MitoCP as well as rotenone, which inhibits the ETC at complex I, proximal to the primary sites of O_2^- generation (41).

Figure 6. (*Continued*). (*C*) Representative confocal images (red, MitoSOX; green, TO-PRO-3 nuclear stain) and (*D*) summary data for MitoSOX fluorescence (mean background-subtracted fluorescence intensity) in primary cultures of rat PASMCs treated with vehicle, PMA (10 μmol/L), or PMA + FSC231 (50 μmol/L). *n* = average of five images from four rats/treatment. (*E* and *G*) Representative confocal images of the Duolink proximity ligation assay (PLA) interaction (red puncta) between goat anti-PKCβI (*E*) or anti-PKCβII (*G*) and rabbit anti-PICK1 in rat PASMCs upon incubation with vehicle or PMA (10 μmol/L). (*F* and *H*) PLA summary data for the average number of puncta per cell. (*I*) Negative controls for PLA experiments in which PASMCs were incubated with both PLA probes and each primary antibody alone or no primary antibody. Actin is labeled with Alexa Fluor 647 Phalloidin (blue) and nuclei are labeled with SyTOX (green). *n* = average of five images from four experiments (rats)/treatment; $^*P < 0.05$ versus vehicle. $^{\#}P < 0.05$ versus PMA alone. Analyzed by unpaired *t* test (*A*, *B*, *F*, and *H*), or one-way ANOVA (*D*). *Post hoc* comparisons were made using the Student-Newman-Keuls test. Scale bars: 25 μm.

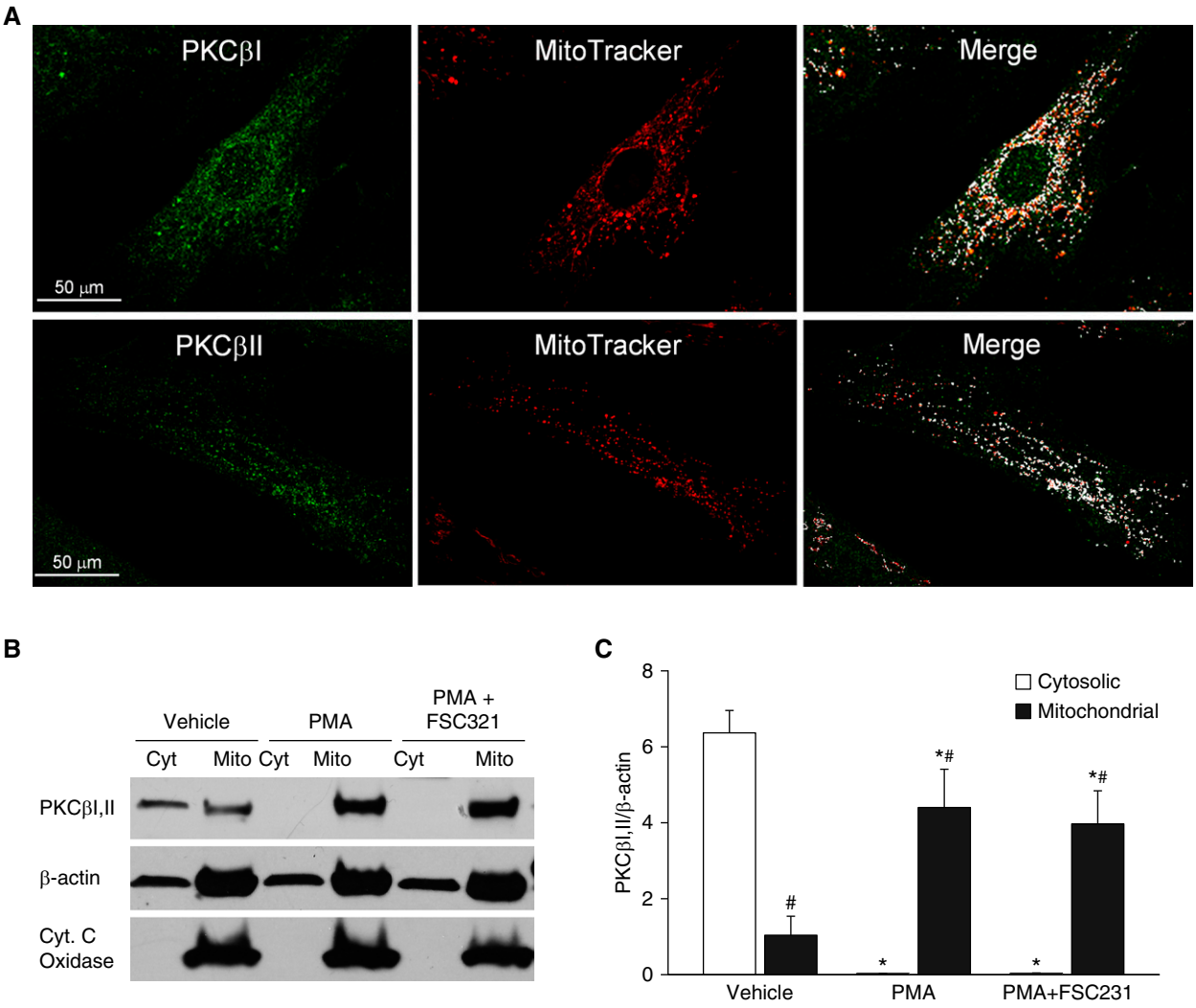

Figure 7. PKCβ undergoes mitochondrial translocation upon stimulation in PASMCs. (*A*) Localization of PKCβI/II to mitochondria in human PASMCs (green, PKCβ immunofluorescence; red, MitoTracker Deep Red; white, colocalization in merged image). (*B*) Representative Western blot for PKCβI/II, cytochrome C (Cyt. C) oxidase (mitochondrial marker), and β-actin in mitochondria (Mito)-enriched and cytosolic (Cyt) fractions from cultured rat PASMCs after treatment with vehicle, PMA (10 μmol/L), or a combination of PMA and the PICK1 inhibitor FSC231 (50 μmol/L). (*C*) Densitometric analysis of Western blots illustrating the effect of PMA to increase PKCβI/II levels (normalized to β-actin) in the mitochondrial fraction, and the lack of effect of PICK1 inhibition on this response. $^{*}P < 0.05$ versus corresponding vehicle. $^{\#}P < 0.05$ versus corresponding cytosolic fraction. $n = 5$ rats/treatment. Analyzed by two-way ANOVA. *Post hoc* comparisons were made using the Student-Newman-Keuls test. Scale bars: 50 μm.

Signaling Relationship between PKCβ and ROS in IH-induced pHTN

We examined whether PKCβ and O_2^- act in a common signaling pathway to mediate vasoconstriction after IH by measuring both ET-1–induced vasoconstriction and O_2^- production in pressurized pulmonary arteries. Consistent with PKCβ and O_2^- acting in series, we found that combined PKCβ inhibition and O_2^- scavenging did not produce additive effects to attenuate constriction in arteries from IH rats. Based on evidence that PKCβ is activated by oxidation (55), and that ROS activate PKCε in PASMCs (56), we hypothesized that mitoROS signal upstream of PKCβ to mediate constriction. However, in contrast to this hypothesis, PKCβ inhibition prevented IH-induced increases in basal and ET-1–mediated O_2^- levels, indicating that PKCβ is required for O_2^- generation in PASMCs from IH rats. In agreement with these results, *in vivo* PKCβ inhibition abolished IH-mediated increases in RVSP and RV hypertrophy, similar to the effects of ROS scavenging. Although these whole-animal studies are limited in that global inhibition of PKCβ and ROS may produce effects independently of PASMC PKCβ and ROS signaling, the consistencies between our *in vivo* and *in vitro* studies argue that PKCβ-dependent ROS production mediates enhanced vasoconstrictor reactivity and pHTN after IH.

Mechanisms of PKCβ-mediated Pulmonary Arterial Constriction

Role of MitoROS. Although PKCβ-mediated pulmonary vasoconstriction becomes linked to ET-1 receptor stimulation only after exposure to IH (14),

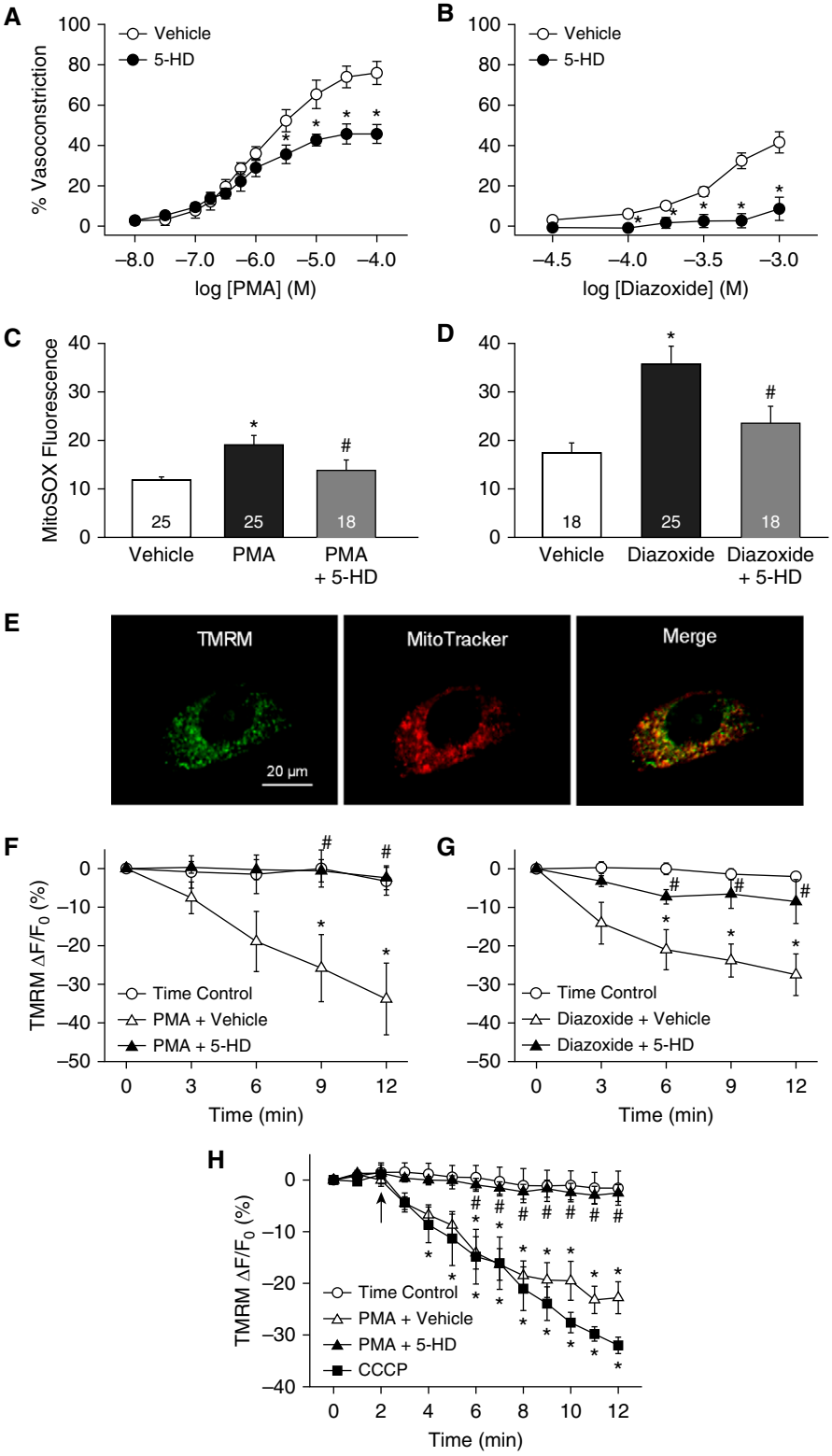

Figure 8. Mitochondrial K_{ATP} (mitoK_{ATP}) channels contribute to PKC-dependent pulmonary vasoconstriction, mitochondrial O_2^- generation, and mitochondrial membrane potential ($\Delta\Psi_M$) depolarization. (*A* and *B*) Vasoconstrictor responses to the PKC agonist PMA (10^{-8} to 10^{-4} mol/L) (*A*) or the mitoK_{ATP} channel activator diazoxide (3×10^{-5} to 10^{-3} mol/L) (*B*) in endothelium-disrupted, pressurized pulmonary arteries from control rats in the presence of the specific mitoK_{ATP}

we found that pharmacological stimulation of PKCβ with PMA mediated constriction of the pulmonary arteries from control animals through a mitoROS-dependent Ca^{2+}-sensitization mechanism. Interestingly, neither PKCβ nor ROS were involved in PMA-dependent constriction of small mesenteric arteries, where PKCβ expression was nearly undetectable, indicating that other PKC isoforms contribute to this response in the mesenteric circulation. These findings demonstrate that PKCβ-induced vasoconstriction is not a generalized phenomenon, and that PKCβ is the predominant isoform mediating PKC-dependent constriction in the pulmonary circulation.

Consistent with vasoreactivity studies, PMA stimulated PKCβ-induced mitoROS production in both human and rat PASMCs, as demonstrated by blockade of mitoROS production after either pharmacologic or shRNA inhibition of PKCβ. This response was associated with acute translocation of PKCβ to mitochondria, similar to previous findings that some PKC isoforms translocate from the cardiac cell membrane to mitochondria in response to ischemia-reperfusion, where they function to increase mitochondrial O_2^- production (57).

Use of PMA is limited by actions of this phorbol ester to nonspecifically stimulate multiple PKC isoforms. Whereas PKCβ inhibition with LY-333531 had no effect on PMA-induced constriction of mesenteric arteries, it nearly abolished reactivity to PMA in pulmonary arteries, supporting a primary contribution of PKCβ to PMA-induced vasoconstriction in the pulmonary circulation. Consistent with these findings, we found that both pharmacologic and genetic inhibition of PKCβ prevented PMA-induced mitoROS generation in pulmonary vascular SMCs. An additional consideration is that long-term treatment with PMA can inhibit PKC activity by downregulating isozyme expression (58). However, our observation that PKC inhibitors attenuated responses to PMA indicate that PMA stimulated, rather than inhibited, PKC.

Role of PICK1. The scaffolding protein PICK1 was originally identified by its ability to bind to the C-terminus of PKC, thereby enhancing enzyme activity (59). PICK1 functions to regulate the activity and

membrane localization of its binding partners by facilitating their interactions with intracellular signaling mediators or by altering their subcellular localization through interactions with membrane lipid domains (27). Considering our previous findings that PICK1 is expressed in PASMCs (25), we hypothesized that PICK1 facilitates PKCβ-dependent mitoROS generation and vasoconstriction by promoting PKCβ localization to the mitochondrial inner membrane. Consistent with this hypothesis, we found that PICK1 inhibition largely attenuated PMA-induced constriction of pulmonary, but not mesenteric, arteries and prevented PMA-dependent increases in mitoROS in rat PASMCs in a manner similar to that observed after PKCβ inhibition. Furthermore, PKC stimulation with PMA increased the colocalization of PICK1 and PKCβII as determined by Duolink PLAs, but had no effect on the association of PICK1 with PKCβI. Although the relative contributions of PKCβI and II to mitoROS-dependent pulmonary vasoconstriction are not clear, these findings are consistent with an effect of PKCβII to functionally interact with PICK1 to mediate this response. Interestingly, subcellular fractionation protocols using an antibody that recognizes both PKCβI and PKCβII demonstrated an acute translocation of PKCβI/II to mitochondria in response to PKC stimulation. However, in contrast to our hypothesis, this response was not altered by PICK1 inhibition, suggesting that PICK1 mediates PKCβ-induced mitoROS production by increasing PKCβ activity or access of the enzyme to relevant phosphorylation targets rather than trafficking PKCβ to mitochondria.

Role of mitoK$_{ATP}$ channels. MitoK$_{ATP}$ channels are structurally distinct from sarcolemmal K$_{ATP}$ channels (28) and are located on the mitochondrial inner membrane. Activation of mitoK$_{ATP}$ channels leads to inward flux of K^+, $\Delta\Psi_M$ depolarization, and ROS generation by the ETC (30). This response mediates multiple oxidative signaling mechanisms, including paradoxical cardioprotection via inhibition of the mitochondrial permeability transition pore in ischemic preconditioning (29), angiotensin II–induced endothelial dysfunction (43), and cerebral artery dilation through activation of Ca^{2+} sparks (42). However, in contrast to these effects of mitoK$_{ATP}$ activation in cerebral arteries, we found that stimulation of mitoK$_{ATP}$ channels with either PMA or diazoxide caused constriction of pulmonary arteries, along with increased production of mitoROS in human PASMCs. Consistent with effects of PMA and diazoxide to activate mitoK$_{ATP}$ channels in these preparations, both agents produced $\Delta\Psi_M$ depolarization in human PASMCs and rat pulmonary arteries that was sensitive to mitoK$_{ATP}$ channel inhibition. These data suggest that PKCβ stimulates mitoROS production through activation of mitoK$_{ATP}$ channels in PASMCs to mediate vasoconstriction. Although the magnitude of this mitoK$_{ATP}$ channel–induced depolarization is somewhat larger than that observed in prior studies (42, 60), these differences may be explained by possible tissue-specific variability in channel expression or differences in the detection sensitivity of the methods employed. Our present findings are in agreement with evidence that PKC-dependent mitoROS generation mediates the cardioprotective effects of mitoK$_{ATP}$ activation (29). MitoK$_{ATP}$ channel activation also contributes to hypoxia-induced $\Delta\Psi_M$ depolarization and proliferation of human PASMCs (61), supporting a possible role for these channels in the arterial remodeling component of hypoxia-associated pHTN.

Challenges for future studies include evaluation of mechanisms by which IH couples receptor stimulation to PKCβ activation in the pulmonary circulation. Oxidative stress can activate PKCβ (55) through reversible oxidation of cysteine thiols located in the autoinhibitory domain of the enzyme (55), producing an increase in catalytic activity and potentiation of agonist-dependent activation. Consequently, PKCβ oxidation resulting from IH-induced paracrine or autocrine oxidant signaling may prime PKCβ for activation by receptor stimulation. It is also possible that PKCβ-induced mitochondrial oxidative stress acts in a feed-forward fashion to further activate the enzyme to promote vascular dysfunction. Therefore, future studies will address the possible role of PKCβ as a redox sensor mediating mitoROS signaling in IH-induced pHTN.

Another unanswered question is how PKCβ-induced mitoROS production mediates contraction independently of changes in PASMC $[Ca^{2+}]_i$. This response does not appear to be result of classical mechanisms of PKC-mediated Ca^{2+}-sensitization involving myosin light chain phosphorylation (14). Considering that dynamic reorganization of the actin cytoskeleton is integral to tension generation in smooth muscle (62), a possible alternative explanation is that ROS-mediated actin polymerization contributes to this response in a manner similar to that which we recently characterized in the pulmonary circulation of chronically hypoxic rats (63).

Conclusions

In conclusion, oxidative stress, increased PASMC Ca^{2+} sensitivity, and elevated

Figure 8. (*Continued*). channel inhibitor 5-hydroxydecanoate (5-HD; 500 μmol/L) or vehicle. Experiments were conducted in the presence of diltiazem (50 μmol/L) to block L-type Ca^{2+} channels. $n = 4$ rats/treatment. $^*P < 0.05$ versus vehicle. (*C* and *D*) Effects of 5-HD (100 μmol/L) on PMA (1 μmol/L)- (*C*) and diazoxide (100 μmol/L)-stimulated MitoSOX fluorescence (*D*) (mean background-subtracted fluorescence intensity) in human PASMCs. $n = 18$–25 images (specified in bars) from three to four experiments/treatment. $^*P < 0.05$ versus vehicle. $^{\#}P < 0.05$ versus PMA or diazoxide. (*E*) Colocalization of the mitochondria-targeted $\Delta\Psi_M$ fluorescent indicator TMRM (100 nmol/L) and MitoTracker Deep Red fluorescence in human PASMCs (green, TMRM; red, MitoTracker). (*F* and *G*) Effects of 5-HD (100 μmol/L) on the percent change in TMRM fluorescence (mean background-subtracted fluorescence intensity) in response to PMA (1 μmol/L) (*F*) or diazoxide (100 μmol/L) in human PASMCs (*G*). This probe accumulates in the mitochondrial matrix as a result of the large negative $\Delta\Psi_M$, and thus fluorescence intensity decreases with $\Delta\Psi_M$ depolarization. $n = 5$–7 experiments/treatment. (*H*) Percent change in TMRM fluorescence in response to PMA (10 μmol/L) in endothelium-disrupted, pressurized pulmonary arteries from control rats in the presence of 5-HD (500 μmol/L) or vehicle. The electron transport chain uncoupler carbonyl cyanide 3-chlorophenylhydrazone (CCCP, 10 μmol/L) was used as a positive control. $n = 4$ rats/treatment for time control, PMA + vehicle, and PMA+5-HD; $n = 3$ for CCCP. (*F* and *G*) $^*P < 0.05$ versus time control. $^{\#}P < 0.05$ versus PMA+vehicle or diazoxide + vehicle. (*A*–*H*) Analyzed by unpaired *t* test (*A* and *B*) or one-way ANOVA (*C*–*H*). *Post hoc* comparisons were made using the Student-Newman-Keuls test. Scale bar: 20 μm.

$[Ca^{2+}]_i$ act as common mediators of pulmonary vasoconstriction in various forms of pHTN. However, the signaling pathways and enzymatic sources of ROS involved in these responses vary considerably depending on the cause of the disease. Whereas NOX-derived ROS and RhoA-mediated Ca^{2+}-sensitization play a critical role in the vasoconstriction and pHTN associated with chronic hypoxia (19, 46), the current findings establish a novel signaling pathway involving PKCβ-induced mitoROS generation that mediates enhanced vasoconstrictor reactivity and pHTN resulting from IH. This signaling mechanism was not observed in mesenteric arteries and thus may be unique to the pulmonary circulation. Furthermore, it is coupled to endothelin receptor stimulation only after IH exposure. Such pulmonary vascular selectivity of this PKCβ pathway could provide an attractive target for pulmonary-selective treatment of IH-induced pHTN that would be distinct from existing strategies used in other forms of pHTN. Future studies are needed to determine the sensing mechanisms that differentiate the effects of chronic hypoxia and IH in the pulmonary circulation, as well as the direct contribution of PKCβ-dependent vasoconstriction to IH-induced pHTN. Considering the protective effects of estradiol in some forms of pHTN (64), it will also be important to investigate whether sex-dependent differences in PKCβ signaling mediate protection of females from IH-induced pHTN. ■

Author disclosures are available with the text of this article at www.atsjournals.org.

Acknowledgment: The authors thank Dr. Navdeep S. Chandel (Department of Medicine, Northwestern University, Chicago, Illinois) for the generous donation of MitoCP, and Eli Lilly and Company (Indianapolis, Indiana) for providing LY-333531.

References

1. Dempsey JA, Veasey SC, Morgan BJ, O'Donnell CP. Pathophysiology of sleep apnea. *Physiol Rev* 2010;90:47–112.
2. Golbin JM, Somers VK, Caples SM. Obstructive sleep apnea, cardiovascular disease, and pulmonary hypertension. *Proc Am Thorac Soc* 2008;5:200–206.
3. Javaheri S, Barbe F, Campos-Rodriguez F, Dempsey JA, Khayat R, Javaheri S, *et al*. Sleep apnea: types, mechanisms, and clinical cardiovascular consequences. *J Am Coll Cardiol* 2017; 69:841–858.
4. Dumitrascu R, Heitmann J, Seeger W, Weissmann N, Schulz R. Obstructive sleep apnea, oxidative stress and cardiovascular disease: lessons from animal studies. *Oxid Med Cell Longev* 2013;2013: 234631.
5. Floras JS. Sleep apnea and cardiovascular disease: an enigmatic risk factor. *Circ Res* 2018;122:1741–1764.
6. Minai OA, Ricaurte B, Kaw R, Hammel J, Mansour M, McCarthy K, *et al*. Frequency and impact of pulmonary hypertension in patients with obstructive sleep apnea syndrome. *Am J Cardiol* 2009;104: 1300–1306.
7. Friedman SE, Andrus BW. Obesity and pulmonary hypertension: a review of pathophysiologic mechanisms. *J Obes* 2012;2012:505274.
8. Kolilekas L, Manali E, Vlami KA, Lyberopoulos P, Triantafillidou C, Kagouridis K, *et al*. Sleep oxygen desaturation predicts survival in idiopathic pulmonary fibrosis. *J Clin Sleep Med* 2013;9:593–601.
9. Shawon MS, Perret JL, Senaratna CV, Lodge C, Hamilton GS, Dharmage SC. Current evidence on prevalence and clinical outcomes of co-morbid obstructive sleep apnea and chronic obstructive pulmonary disease: a systematic review. *Sleep Med Rev* 2017;32:58–68.
10. Campen MJ, Shimoda LA, O'Donnell CP. Acute and chronic cardiovascular effects of intermittent hypoxia in C57BL/6J mice. *J Appl Physiol (1985)* 2005;99:2028–2035.
11. Fagan KA. Selected contribution: pulmonary hypertension in mice following intermittent hypoxia. *J Appl Physiol (1985)* 2001;90: 2502–2507.
12. Nisbet RE, Graves AS, Kleinhenz DJ, Rupnow HL, Reed AL, Fan TH, *et al*. The role of NADPH oxidase in chronic intermittent hypoxia-induced pulmonary hypertension in mice. *Am J Respir Cell Mol Biol* 2009;40:601–609.
13. Norton CE, Jernigan NL, Kanagy NL, Walker BR, Resta TC. Intermittent hypoxia augments pulmonary vascular smooth muscle reactivity to NO: regulation by reactive oxygen species. *J Appl Physiol (1985)* 2011;111:980–988.
14. Snow JB, Gonzalez Bosc LV, Kanagy NL, Walker BR, Resta TC. Role for PKCβ in enhanced endothelin-1-induced pulmonary vasoconstrictor reactivity following intermittent hypoxia. *Am J Physiol Lung Cell Mol Physiol* 2011;301:L745–L754.
15. Snow JB, Kitzis V, Norton CE, Torres SN, Johnson KD, Kanagy NL, *et al*. Differential effects of chronic hypoxia and intermittent hypocapnic and eucapnic hypoxia on pulmonary vasoreactivity. *J Appl Physiol (1985)* 2008;104:110–118.
16. Chi AY, Waypa GB, Mungai PT, Schumacker PT. Prolonged hypoxia increases ROS signaling and RhoA activation in pulmonary artery smooth muscle and endothelial cells. *Antioxid Redox Signal* 2010;12: 603–610.
17. Fagan KA, Oka M, Bauer NR, Gebb SA, Ivy DD, Morris KG, *et al*. Attenuation of acute hypoxic pulmonary vasoconstriction and hypoxic pulmonary hypertension in mice by inhibition of Rho-kinase. *Am J Physiol Lung Cell Mol Physiol* 2004;287: L656–L664.
18. Jernigan NL, Walker BR, Resta TC. Reactive oxygen species mediate RhoA/Rho kinase-induced Ca^{2+} sensitization in pulmonary vascular smooth muscle following chronic hypoxia. *Am J Physiol Lung Cell Mol Physiol* 2008;295:L515–L529.
19. Nagaoka T, Morio Y, Casanova N, Bauer N, Gebb S, McMurtry I, *et al*. Rho/Rho kinase signaling mediates increased basal pulmonary vascular tone in chronically hypoxic rats. *Am J Physiol Lung Cell Mol Physiol* 2004;287:L665–L672.
20. Weigand L, Sylvester JT, Shimoda LA. Mechanisms of endothelin-1-induced contraction in pulmonary arteries from chronically hypoxic rats. *Am J Physiol Lung Cell Mol Physiol* 2006;290: L284–L290.
21. Norton CE, Sheak JR, Yan S, Weise-Cross L, Jernigan NL, Walker BR, *et al*. Augmented pulmonary vasoconstrictor reactivity after chronic hypoxia requires Src kinase and epidermal growth factor receptor signaling. *Am J Respir Cell Mol Biol* 2020;62:61–73.
22. Soliman H, Gador A, Lu YH, Lin G, Bankar G, MacLeod KM. Diabetes-induced increased oxidative stress in cardiomyocytes is sustained by a positive feedback loop involving Rho kinase and PKCβ2. *Am J Physiol Heart Circ Physiol* 2012;303:H989–H1000.
23. Wang G, Chen Z, Zhang F, Jing H, Xu W, Ning S, *et al*. Blockade of PKCβ protects against remote organ injury induced by intestinal ischemia and reperfusion via a p66shc-mediated mitochondrial apoptotic pathway. *Apoptosis* 2014;19:1342–1353.
24. McNicholas WT. Chronic obstructive pulmonary disease and obstructive sleep apnea: overlaps in pathophysiology, systemic inflammation, and cardiovascular disease. *Am J Respir Crit Care Med* 2009;180:692–700.
25. Herbert LM, Nitta CH, Yellowhair TR, Browning C, Gonzalez Bosc LV, Resta TC, *et al*. PICK1/calcineurin suppress ASIC1-mediated Ca^{2+} entry in rat pulmonary arterial smooth muscle cells. *Am J Physiol Cell Physiol* 2016;310:C390–C400.
26. Thorsen TS, Madsen KL, Rebola N, Rathje M, Anggono V, Bach A, *et al*. Identification of a small-molecule inhibitor of the PICK1 PDZ domain that inhibits hippocampal LTP and LTD. *Proc Natl Acad Sci USA* 2010;107:413–418.

27. Wang WL, Yeh SF, Chang YI, Hsiao SF, Lian WN, Lin CH, *et al*. PICK1, an anchoring protein that specifically targets protein kinase Calpha to mitochondria selectively upon serum stimulation in NIH 3T3 cells. *J Biol Chem* 2003;278:37705–37712.
28. Foster DB, Ho AS, Rucker J, Garlid AO, Chen L, Sidor A, *et al*. Mitochondrial ROMK channel is a molecular component of mitoK(ATP). *Circ Res* 2012;111:446–454.
29. Garlid AO, Jaburek M, Jacobs JP, Garlid KD. Mitochondrial reactive oxygen species: which ROS signals cardioprotection? *Am J Physiol Heart Circ Physiol* 2013;305:H960–H968.
30. Costa AD, Quinlan CL, Andrukhiv A, West IC, Jabůrek M, Garlid KD. The direct physiological effects of mitoK(ATP) opening on heart mitochondria. *Am J Physiol Heart Circ Physiol* 2006;290:H406–H415.
31. Chopra S, Polotsky VY, Jun JC. Sleep apnea research in animals: past, present, and future. *Am J Respir Cell Mol Biol* 2016;54:299–305.
32. Allahdadi KJ, Cherng TW, Pai H, Silva AQ, Walker BR, Nelin LD, *et al*. Endothelin type A receptor antagonist normalizes blood pressure in rats exposed to eucapnic intermittent hypoxia. *Am J Physiol Heart Circ Physiol* 2008;295:H434–H440.
33. Jernigan NL, Naik JS, Weise-Cross L, Detweiler ND, Herbert LM, Yellowhair TR, *et al*. Contribution of reactive oxygen species to the pathogenesis of pulmonary arterial hypertension. *PLoS One* 2017; 12:e0180455.
34. Jirousek MR, Gillig JR, Gonzalez CM, Heath WF, McDonald JH III, Neel DA, *et al*. (S)-13-[(dimethylamino)methyl]-10,11,14,15-tetrahydro-4,9: 16, 21-dimetheno-1H, 13H-dibenzo[e,k]pyrrolo[3,4-h][1,4,13] oxadiazacyclohexadecene-1,3(2H)-d ione (LY333531) and related analogues: isozyme selective inhibitors of protein kinase C β. *J Med Chem* 1996;39:2664–2671.
35. Harja E, Chang JS, Lu Y, Leitges M, Zou YS, Schmidt AM, *et al*. Mice deficient in PKCbeta and apolipoprotein E display decreased atherosclerosis. *FASEB J* 2009;23:1081–1091.
36. Chen SJ, Chen YF, Meng QC, Durand J, Dicarlo VS, Oparil S. Endothelin-receptor antagonist bosentan prevents and reverses hypoxic pulmonary hypertension in rats. *J Appl Physiol (1985)* 1995; 79:2122–2131.
37. Norton CE, Broughton BR, Jernigan NL, Walker BR, Resta TC. Enhanced depolarization-induced pulmonary vasoconstriction following chronic hypoxia requires EGFR-dependent activation of NAD(P)H oxidase 2. *Antioxid Redox Signal* 2013;18:1777–1788.
38. Plomaritas DR, Herbert LM, Yellowhair TR, Resta TC, Gonzalez Bosc LV, Walker BR, *et al*. Chronic hypoxia limits H_2O_2-induced inhibition of ASIC1-dependent store-operated calcium entry in pulmonary arterial smooth muscle. *Am J Physiol Lung Cell Mol Physiol* 2014; 307:L419–L430.
39. Dhanasekaran A, Kotamraju S, Karunakaran C, Kalivendi SV, Thomas S, Joseph J, *et al*. Mitochondria superoxide dismutase mimetic inhibits peroxide-induced oxidative damage and apoptosis: role of mitochondrial superoxide. *Free Radic Biol Med* 2005;39:567–583.
40. Jiang J, Stoyanovsky DA, Belikova NA, Tyurina YY, Zhao Q, Tungekar MA, *et al*. A mitochondria-targeted triphenylphosphonium-conjugated nitroxide functions as a radioprotector/mitigator. *Radiat Res* 2009;172:706–717.
41. Bell EL, Klimova TA, Eisenbart J, Moraes CT, Murphy MP, Budinger GR, *et al*. The Qo site of the mitochondrial complex III is required for the transduction of hypoxic signaling via reactive oxygen species production. *J Cell Biol* 2007;177:1029–1036.
42. Xi Q, Cheranov SY, Jaggar JH. Mitochondria-derived reactive oxygen species dilate cerebral arteries by activating Ca^{2+} sparks. *Circ Res* 2005;97:354–362.
43. Doughan AK, Harrison DG, Dikalov SI. Molecular mechanisms of angiotensin II-mediated mitochondrial dysfunction: linking mitochondrial oxidative damage and vascular endothelial dysfunction. *Circ Res* 2008;102:488–496.
44. Gerencser AA, Chinopoulos C, Birket MJ, Jastroch M, Vitelli C, Nicholls DG, *et al*. Quantitative measurement of mitochondrial membrane potential in cultured cells: calcium-induced de- and hyperpolarization of neuronal mitochondria. *J Physiol* 2012;590:2845–2871.
45. Loor G, Kondapalli J, Iwase H, Chandel NS, Waypa GB, Guzy RD, *et al*. Mitochondrial oxidant stress triggers cell death in simulated ischemia-reperfusion. *Biochim Biophys Acta* 2011;1813:1382–1394.
46. Liu JQ, Zelko IN, Erbynn EM, Sham JS, Folz RJ. Hypoxic pulmonary hypertension: role of superoxide and NADPH oxidase (gp91phox). *Am J Physiol Lung Cell Mol Physiol* 2006;290:L2–L10.
47. Nozik-Grayck E, Stenmark KR. Role of reactive oxygen species in chronic hypoxia-induced pulmonary hypertension and vascular remodeling. *Adv Exp Med Biol* 2007;618:101–112.
48. Knock GA, Snetkov VA, Shaifta Y, Connolly M, Drndarski S, Noah A, *et al*. Superoxide constricts rat pulmonary arteries via Rho-kinase-mediated Ca(2+) sensitization. *Free Radic Biol Med* 2009;46:633–642.
49. Fike CD, Slaughter JC, Kaplowitz MR, Zhang Y, Aschner JL. Reactive oxygen species from NADPH oxidase contribute to altered pulmonary vascular responses in piglets with chronic hypoxia-induced pulmonary hypertension. *Am J Physiol Lung Cell Mol Physiol* 2008;295:L881–L888.
50. Fike CD, Aschner JL, Slaughter JC, Kaplowitz MR, Zhang Y, Pfister SL. Pulmonary arterial responses to reactive oxygen species are altered in newborn piglets with chronic hypoxia-induced pulmonary hypertension. *Pediatr Res* 2011;70:136–141.
51. Heumüller S, Wind S, Barbosa-Sicard E, Schmidt HH, Busse R, Schröder K, *et al*. Apocynin is not an inhibitor of vascular NADPH oxidases but an antioxidant. *Hypertension* 2008;51: 211–217.
52. Waypa GB, Marks JD, Guzy RD, Mungai PT, Schriewer JM, Dokic D, *et al*. Superoxide generated at mitochondrial complex III triggers acute responses to hypoxia in the pulmonary circulation. *Am J Respir Crit Care Med* 2013;187:424–432.
53. Rathore R, Zheng YM, Niu CF, Liu QH, Korde A, Ho YS, *et al*. Hypoxia activates NADPH oxidase to increase [ROS]i and $[Ca^{2+}]_i$ through the mitochondrial ROS-PKCepsilon signaling axis in pulmonary artery smooth muscle cells. *Free Radic Biol Med* 2008;45: 1223–1231.
54. Muller FL, Liu Y, Van Remmen H. Complex III releases superoxide to both sides of the inner mitochondrial membrane. *J Biol Chem* 2004; 279:49064–49073.
55. Giorgi C, Agnoletto C, Baldini C, Bononi A, Bonora M, Marchi S, *et al*. Redox control of protein kinase C: cell- and disease-specific aspects. *Antioxid Redox Signal* 2010;13:1051–1085.
56. Rathore R, Zheng YM, Li XQ, Wang QS, Liu QH, Ginnan R, *et al*. Mitochondrial ROS-PKCepsilon signaling axis is uniquely involved in hypoxic increase in $[Ca^{2+}]_i$ in pulmonary artery smooth muscle cells. *Biochem Biophys Res Commun* 2006;351:784–790.
57. Churchill EN, Szweda LI. Translocation of deltaPKC to mitochondria during cardiac reperfusion enhances superoxide anion production and induces loss in mitochondrial function. *Arch Biochem Biophys* 2005;439:194–199.
58. Wang Y, Zhou H, Wu B, Zhou Q, Cui D, Wang L. Protein kinase C isoforms distinctly regulate propofol-induced endothelium-dependent and endothelium-independent vasodilation. *J Cardiovasc Pharmacol* 2015;66:276–284.
59. Staudinger J, Zhou J, Burgess R, Elledge SJ, Olson EN. PICK1: a perinuclear binding protein and substrate for protein kinase C isolated by the yeast two-hybrid system. *J Cell Biol* 1995;128: 263–271.
60. Laskowski M, Augustynek B, Kulawiak B, Koprowski P, Bednarczyk P, Jarmuszkiewicz W, *et al*. What do we not know about mitochondrial potassium channels? *Biochim Biophys Acta* 2016;1857:1247–1257.
61. Hu HL, Zhang ZX, Chen CS, Cai C, Zhao JP, Wang X. Effects of mitochondrial potassium channel and membrane potential on hypoxic human pulmonary artery smooth muscle cells. *Am J Respir Cell Mol Biol* 2010;42:661–666.
62. Gunst SJ, Zhang W. Actin cytoskeletal dynamics in smooth muscle: a new paradigm for the regulation of smooth muscle contraction. *Am J Physiol Cell Physiol* 2008;295:C576–C587.
63. Weise-Cross L, Sands MA, Sheak JR, Broughton BRS, Snow JB, Gonzalez Bosc LV, *et al*. Actin polymerization contributes to enhanced pulmonary vasoconstrictor reactivity after chronic hypoxia. *Am J Physiol Heart Circ Physiol* 2018;314:H1011–H1021.
64. Resta TC, Kanagy NL, Walker BR. Estradiol-induced attenuation of pulmonary hypertension is not associated with altered eNOS expression. *Am J Physiol Lung Cell Mol Physiol* 2001;280: L88–L97.